electronics

MDPI

Article

Stability Analysis of Power Hardware-in-the-Loop Simulations for Grid Applications

Simon Resch *, Juliane Friedrich, Timo Wagner, Gert Mehlmann and Matthias Luther

Institute of Electrical Energy Systems, Friedrich-Alexander University Erlangen-Nürnberg, Cauerstraße 4, 91058 Erlangen, Germany; juliane.f.friedrich@fau.de (J.F.); timo.wagner@fau.de (T.W.); gert.mehlmann@fau.de (G.M.); matthias.luther@fau.de (M.L.)

* Correspondence: simon.resch@fau.de (S.R.)

Abstract: Power Hardware-in-the-Loop (PHiL) simulation is an emerging testing methodology of real hardware equipment within an emulated virtual environment. The closed loop interfacing between the Hardware under Test (HuT) and the Real Time Simulation (RTS) enables a realistic simulation but can also result in an unstable system. In addition to fundamentals in PHiL simulation and interfacing, this paper therefore provides a consistent and comprehensive study of PHiL stability. An analytic analysis is compared with a simulative approach and is supplemented by practical validations of the stability limits in PHiL simulation. Special focus is given on the differences between a switching and a linear amplifier as power interface (PI). Stability limits and the respective factors of influence (e.g., Feedback Current Filtering) are elaborated with a minimal example circuit with voltage-type Ideal Transformer Model (ITM) PHiL interface algorithm (IA). Finally, the findings are transferred to a real low-voltage grid PHiL application with residential load and photovoltaic system.

Keywords: power hardware-in-the-loop; real time simulation; interface algorithm; ideal transformer model; feedback current filtering; PHiL stability; linear/switching amplifier

check for updates

Citation: Resch, S.; Friedrich, J.; Wagner, T.; Mehlmann, G.; Luther, M. Stability Analysis of Power Hardware-in-the-Loop Simulations for Grid Applications. *Electronics* **2022**, *11*, 7. https://doi.org/10.3390/electronics11010007

Academic Editors: Miro Milanovic, Enric Vidal Idiarte and Eric Monmasson

Received: 24 November 2021
Accepted: 16 December 2021
Published: 21 December 2021

Publisher's Note: MDPI stays neutral with regard to jurisdictional claims in published maps and institutional affiliations.

1. Introduction

A drastic reduction of greenhouse gas emissions in the energy sector requires a fundamental transition of energy supply [1]. The transformation of the electrical grid to integrate a vast amount of fluctuating renewable energy systems (RES) plays a key role on the way to a low-carbon society. However, this implicates new challenges for the existing energy system with the requirement of new market structures, closer communicative networking and new technological solutions [2]. The increasing complexity also demands for more comprehensive testing possibilities of new equipment [3,4]. The impact of the increasing penetration of the electrical energy system with power electronic converters requires more detailed modeling together with an in-depth consideration of converter control. Real Time Simulation (RTS), and Power Hardware-in-the-Loop (PHiL) in particular, will therefore play an increasing role in the validation and testing process of new systems and equipment in order to fully investigate its behavior in a flexible and realistic environment [3].

In the last decade a lot of research on PHiL simulation has been performed. Among others, stability analysis of a PHiL simulation at a theoretical basis is shown in [3,5–13] however, Refs. [7,10,11] solely focus on real impedance. In [6] complex impedances are also considered together with experimental validations, although without a quantitative analysis of the stability limits. Experimental validations of PHiL stability criteria with a linear power amplifier as power interface (PI) are shown in [6,10,14] whereas switching inverters are applied in [11,15]. However, to the knowledge of the author, no work has been done that explicitly applies PHiL stability theory to directly compare linear and switching inverters with the same real-time model and hardware setup.

Therefore, the focus of this paper is a consistent analysis of PHiL stability from theoretical considerations over a simulative approach to practical validations investigating

the stability limit. Due to the fact that both switching and linear inverters are common in different laboratories, but behave differently, stability is shown for both converter types. In the context of this research, the following work is done:

- A general analysis of PHiL stability based on the transfer function of a simplified circuit. The influence of impedance ratio, time delay, amplifier characteristics and low-pass filtering has been considered.
- An offline model of an exemplary PHiL simulation case was implemented in MATLAB Simulink™. Applying the findings of the theoretical analysis, the limits of stable PHiL simulation have been systematically investigated. Both, interfacing with a switching and a linear amplifier has been analyzed with a modeling approach.
- The modeling approach is validated with a real PHiL laboratory setup with both a linear and a switching amplifier in comparison.
- The results are applied to the example of a PV system with a residential load at the low-voltage grid to ensure stability in a real PHiL application.

Alongside with the analytic, simulative and experimental stability analysis, a brief introduction on the basic idea of RTS and the fundamentals of PHiL simulation techniques are explained in Chapter 2 as well as a presentation of the laboratory structures used in this work. The rest of the paper is structured as follows: In Chapter 3 the influencing factors on the stability of a PHiL simulation are analyzed based on an analytic approach. The findings are transferred to a simulative PHiL model and are experimentally validated in Chapter 4 with respect to the differences between linear and switching PI. Chapter 5 presents mitigation of an unstable PHiL simulation at the example of a real application by applying the findings of the previous sections. The results of the stability analysis and the deviations between the theoretical and experimental results are discussed in Chapter 6. A detailed summery along with the key findings of the research work is given in Chapter 7.

2. Power Hardware-in-the-Loop Simulation of Electrical Energy Systems

Hardware-in-the-loop (HiL) simulation provides flexibility to a laboratory installation and the possibility of testing at an early stage of development in a realistic environment.

In that way, physical components can be virtually coupled to any suitable grid with the possibility of freely adapting grid parameters. Thus, the behavior of an equipment at abnormal grid conditions can be examined in detail with reproducible results. Grid impact of new control or protection algorithms at an early stage of development can be tested with real hardware. Furthermore, new equipment can be implemented as a real-time model before prototyping to test the behavior within a real grid in a cost-effective way in an early stage of development [16–18].

HiL simulation is used whenever a single component or a part of a larger system shall be investigated in a realistic environment, especially if a laboratory setup of the whole system is not possible due to economic or technical reasons. HiL can be divided in Power Hardware-in-the-loop (PHiL) and Control-Hardware-in-the-loop (CHiL). The latter describes the interfacing of a real physical controller, protection relay or software within a simulated environment, e.g., RTS of an electrical grid. The interfacing between the RTS and the device under test is established via low-voltage analog signals or network communication protocols [19,20].

PHiL in contrary integrates physical power equipment into a real-time model of an electrical grid, resp., parts of an electrical grid. Amplification of the RTS signals to provide sufficient voltage level and currents for operation of the hardware is needed. However, the setup of an accurate and stable PHiL simulation is not straightforward [3], which will be shown in the context of this paper.

Different abbreviations are customary for the real physical equipment. Device under Test (DuT) [8,21], Equipment under Test (EuT) [20] or Physical Power System (PPS) [18] are seldom used. In contrast, Hardware under Test (HuT), is most common [6,13–16,20,22–25], therefore this abbreviation will be used in this paper. The virtual part of the system which

has to be modeled and simulated in real time will be referred to as Real Time Simulation (RTS) in the following.

2.1. Real Time Simulation

Through significant improvements in CPU performance in the last decades, real-time-simulators now provide the ability to calculate even large power systems within microseconds [26,27]. This enables electromagnetic transient (emt)-simulation in real time. A realistic representation of the dynamics of a system in the discrete time domain requires sufficiently small simulation time steps [22,27,28]. Thus, real time in this context means:

1. The fixed simulation time step has to be small enough to resolve even transients with sufficient accuracy;
2. All calculations for a simulation time step, as well as the signal input and output, must be completed within the time period corresponding to the real time.

RTS is used whenever there is an interaction between a system operating at real-world speed and a model. With an offline simulation the computation time will rise with increased complexity of the model. Thus, a specific period of time in an offline simulation can be slower or faster than real-world time. Offline simulation programs often use variable time steps to increase accuracy around fast changing events or discontinuities [29]. However, digital RTS rely on fixed time steps. Each time step has to be solved during the time span that equals the real-world time which requires powerful processors [26].

Established RTS processors can simulate with time steps in the range of micro to milliseconds, whereas FPGA based simulators achieve even sub-microsecond simulation time steps [4].

2.2. RTS-PHiL Laboratories

In the *Real Time Laboratory*, the Institute of Electrical Energy Systems (LEES) therefore controls multiple real-time simulators from different manufacturers. In this work a *NovaCor™* simulator from *RTDS Technologies Inc., Winnipeg, Canada* is used.

The Real Time Laboratory is coupled via optical fiber connections to the *Microgrid, Energy Storage and Power Hardware-in-the-Loop Laboratory* of the LEES. The laboratory is operated as a campus type microgrid with PHiL capabilities. The microgrid integrates battery storage systems (BSS) of different types, including a 15 kWh/5 kVA vanadium-redox-flow storage system as well as a 4 kWh/4, 6 kVA lead-acid BSS and multiple lithium-ion based BSSs with a total of 82 kWh. It is supplied by a rooftop photovoltaics (PV) system of 17.42 kW rated power. A microgrid-controller for energy management is implemented on an industrial standard automation unit. Details can be extracted from [30,31]. Real-time digital simulators are not able to handle high voltage and currents. Therefore a power amplifier is required for interconnection of the RTS and the HuT. The laboratory is equipped with two three-phase four-quadrant amplifiers (4QA). A 4QA linear amplifier with a source and sink capability of 15 kVA and a 4QA switching inverter with a nominal rated power of 45 kVA with energy recovery capability. A schema of the laboratories is illustrated in Figure 1.

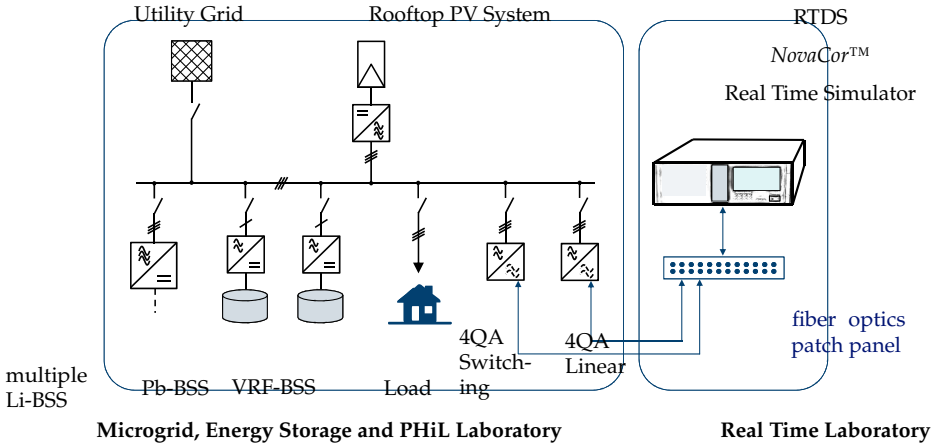

Figure 1. Setup of the *Microgrid, Energy Storage and Power Hardware-in-the-Loop Laboratory* in collaboration with the *Real Time Laboratory* of the LEES.

2.3. PHiL Simulation Fidelity and Errors

The division of an electrical grid into a simulated section and a hardware section implies the need for an interface. Inevitably, however, this will lead to a certain time delay between the two parts and to the introduction of noise into the system. These errors influence stability and accuracy of the PHiL simulation [3,15,19,23]. Figure 2 provides an overview of the effects that influence accuracy and therefore can result in stability issues. The power interface provides non-ideal behavior, and thus introduces time delays, limited bandwidth, set-point deviations and measurement noise [5,32]. Eventually additional hardware is included in the circuit as inverter output filters. Another cause of error is the RTS itself which introduces a time delay through discrete time step simulation [5]. In addition the coupling between the RTS and the PI can introduce errors through communication time delays, limited bandwidth or through noise that is injected when using analog communication [5,32]. The PI and the RTS both operate at a specific sample time. If there is no time synchronization, variable delays occur which introduce harmonics and noise in the system [4] (see Section 3.2.3).

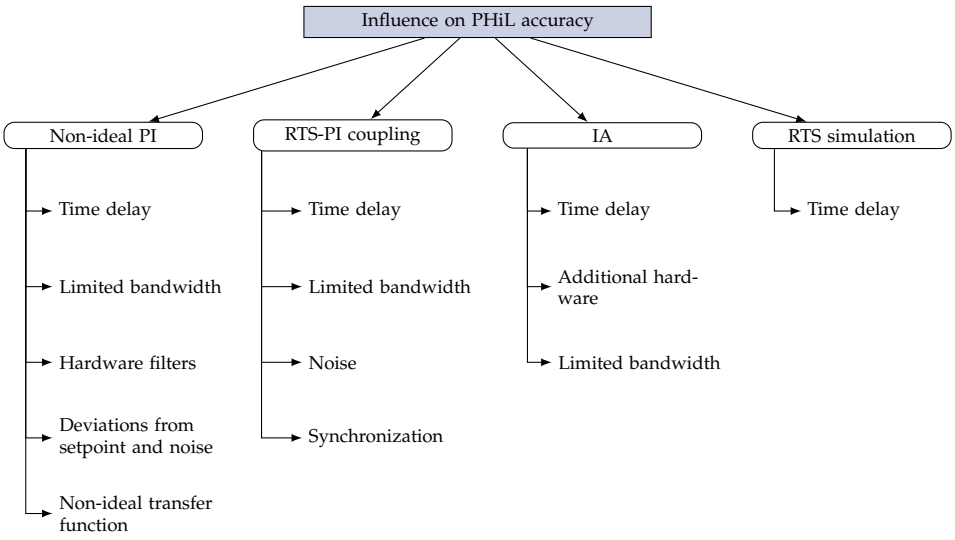

Figure 2. Major accuracy deviations that are introduced in a system through PHiL simulation.

In addition, several IAs are known to improve PHiL stability [3]. However, IAs also introduce deviations from the ideal PHiL simulation by additional time delays, band limitation or extra hardware as stabilizing elements (see Section 2.6). Further details on accuracy with different IAs can be found in [3,5,8].

2.4. PHiL Power Interface

PHiL imposes the need for an amplifier as power interface (PI) to provide the voltage, resp., currents from the RTS at the HuT at an applicable level. In dependence on the application source and sink capability may be required. Four-quadrant operation of the PI is described as an independent control of positive and negative current and voltage and therefore an independent source and sink of real and reactive power [33].

A distinguishing feature of the PI is the converter technology that can be classified into switching and linear amplifiers. Linear amplifiers operate in the linear region of the semiconductors (e.g., linear-MOSFET), whereas switching converters are approaching the desired output voltage and current by high-frequency PWM which implicates the necessity of complex control loops and amplifier output filters [24].

The main advantages of linear amplifiers are small time delays and a wide frequency bandwidth [5,33,34]. The downside of linear amplifiers are high energy losses, up to one-third [33]. In comparison switching amplifiers provide efficiencies over 90 %, are more economical and smaller in size [33,34]. However, a stable PHiL simulation may be more difficult to archive due to increased time delays and nonlinear behavior [5].

2.5. Communication between RTS and PI

The communication between the real time simulator and the PI is bidirectional. Interfacing can be implemented with analog signals or by digital communication protocols. For analog interfacing D/A and A/D converters are needed [11]. The induction of noise has to be prevented and galvanic isolation of simulator and PI is recommended [33]. Digital communication through fiber optics avoids noise and ground-loop problems and provides a fast broadband communication [33]. In this work the communication between the real time simulator and the amplifier is implemented with digital optical fiber AURORA communication protocol.

2.6. Interfacing Algorithms

Closed loop PHiL is characterized by mutual interaction between RTS and HuT. The interfacing therefore is crucial regarding stability and simulation accuracy [3]. With the IA it is specified, which values are being transmitted (e.g., voltage, current, power, torque, etc.) and how the signals are being processed (e.g., unity gain, low-pass-filtered, lead-lag compensator, etc.) [15].

The different IAs each have their own advantages and disadvantages. Therefore, a combination of different IAs is often used in order to achieve the best possible results [3]. The following section presents several different IAs and methods of enhancing the stability of a PHiL simulation.

2.6.1. Ideal Transformer Model (ITM)

The Ideal Transformer Model (ITM) algorithm (also called Ideal Transfer Model or Ideal Transformer Method [14,18]) is the most straightforward IA and very well established. It can be implemented as a voltage controlled variant or as a current controlled variant. For the voltage-type ITM, which is depicted in Figure 3, the reference voltage of the RTS is sent to the PI that forms the voltage at the HuT. This produces a current through the HuT which is measured and fed back to the RTS. For the current-type ITM the current of the RTS is amplified by the PI while the voltage across the HuT is used as feedback signal. The ITM IA offers high accuracy and has the benefit that no further hardware is needed. However, stability issues can be more challenging than in comparison with other interfacing algorithms [15].

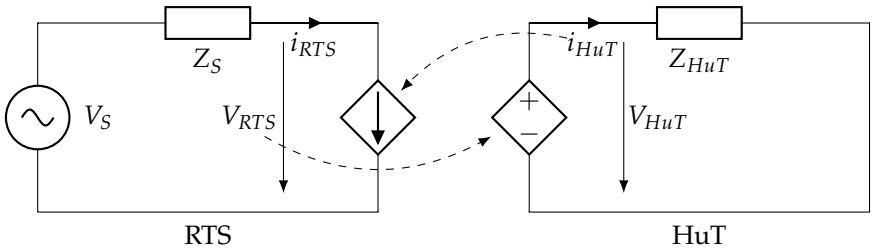

Figure 3. Voltage-type ITM interfacing algorithm for PHiL simulation.

2.6.2. Partial Circuit Duplication (PCD)

The PCD algorithm involves a linking component Z_{ab}, which is repeated in both RTS and the HuT, as illustrated in Figure 4. The larger the value of the linking impedance, the higher the stability of the system. However, with a higher value of Z_{ab} the accuracy decreases due to increased power losses [15]. Note that feedback from the HuT is implemented by a controlled voltage source in the RTS. In [35] detailed discussion of the PCD algorithm is provided.

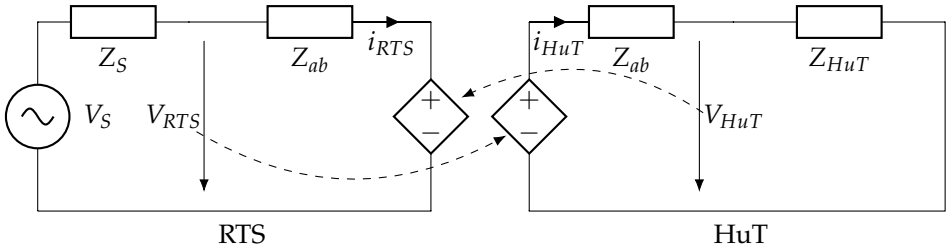

Figure 4. PCD interfacing algorithm for PHiL simulation.

2.6.3. Damping Impedance Model (DIM)

The DIM algorithm consists of a combination of ITM and PCD techniques. It requires a linking impedance Z_{ab} as well as a damping impedance Z^*. Its schematic is depicted in Figure 5. This method leads to absolutely stable results if Z^* is equal to the impedance of the HuT Z_{HuT}. In reality, the knowledge of the exact value of Z_{HuT} requires a perfect model of the HuT which is usually not available. Furthermore, it would make the PHiL simulation dispensable. Nevertheless, high stability margins and good accuracy can still be achieved with the DIM-Algorithm if Z^* is close to the actual value of the hardware impedance [15].

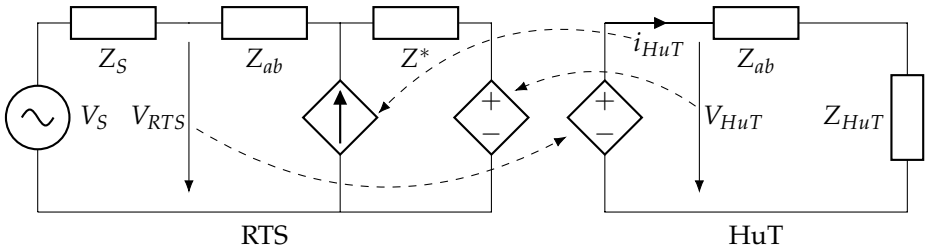

Figure 5. DIM interfacing algorithm for PHiL simulation.

2.6.4. Transmission Line Model (TLM)

The TLM algorithm involves a reactive linking component Z_{lk}, which is considered as a Bergeron transmission line section and modeled as an equivalent Norton or Thévenin circuit. This algorithm is commonly used for decoupling large systems with sufficiently long transmission lines for the benefit of parallel computation. It offers high stability given that it is numerically based on the trapezoidal approximation. However, it might lead to some drawbacks such as large power consumption, low flexibility and high maintenance cost [15,36].

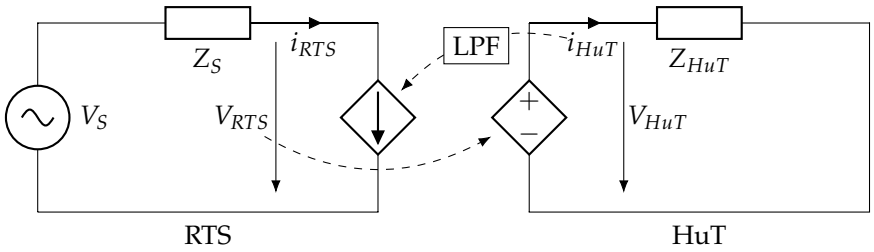

Figure 6. Voltage-type ITM with FSF.

2.6.5. Hardware Inductance Addition Method (HIA)

The HIA-method can be applied to voltage-type interfaces. It involves an additional inductance L_{ADD}, which is added to the hardware side. L_{ADD} is connected in series with the HuT and leads to an improvement in stability but also to a decrease in accuracy [3].

2.6.6. Feedback Signal Filtering (FSF)

FSF applies a low-pass filter to the feedback signal. Figure 6 illustrates the Feedback Current Filtering Method (FCF) at the example of the voltage type ITM algorithm. The filter improves the stability of the system. It can be implemented analogue or in software. For this reason, further hardware is not necessarily needed. Its influence on the stability and accuracy of the simulation depends on the cut-off frequency of the filter [37]. FSF can also be combined with other IAs [3].

2.6.7. Further Interfacing Algorithms

Other possible interfacing algorithms are the Time-variant First-order Approximation (TFA) which is discussed in [15] and the Taganrog Algorithm. A description of the Taganrog Algorithm can be found in [35]. The Multi-Rate Partitioning Method (MRP) and the Partial Shifting Impedance (PSI) are—like HIA and FSF—further methods of improving the stability of a PHiL simulation. [3] presents an overview of these methods.

3. Analytic Approach to PHiL Stability

In this section the stability of a PHiL simulation is investigated analytically. To keep the analysis as comprehensible as possible a minimal example of a PHiL setup is introduced in Section 3.1. In Section 3.2 the stability of a PHiL simulation is analyzed by applying Nyquist stability criterion (NSC) to the open loop transfer function (OLTF). Subsequently the findings are compared with an emt simulation in MATLAB Simulink™ and an experimental setup in the following chapter (Section 4) to validate the analytic approach.

3.1. Minimal PHiL example circuit

To analyze the influencing parameters on PHiL stability an exemplary section of a low-voltage grid shall be reduced to a simple, single-phase circuit. An ideal voltage source V_S with equivalent impedance Z_S represents a low voltage distribution grid as depicted in Figure 7 and the impedance Z_{HuT} represents a residential load.

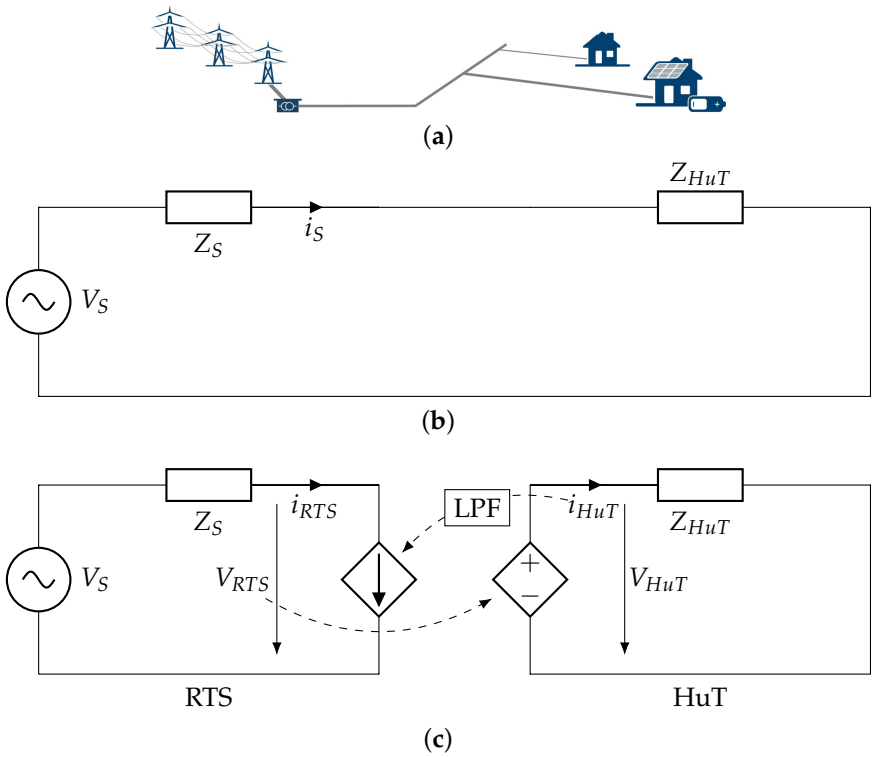

Figure 7. Exemplary low-voltage grid reduced to a minimal PHiL circuit with voltage-type ITM IA (**a**) Exemplary low-voltage grid; (**b**) Simplified equivalent circuit of the low-voltage grid; (**c**) Equivalent circuit with voltage-type ITM IA.

The circuit in Figure 7 can be split into a virtual model and a physical part. An active HuT (e.g., a power electronics inverter or a generator supplying the grid) can be represented as an additional voltage or current source within the HuT, which is shown in [8,37]. In case the circuit includes nonlinearities, the following stability criterion is not applicable without simplification. This issue is addressed in [14,15]. For simplicity, the HuT is therefore considered as a passive, linear system in this work.

In general, the impedance on the RTS side Z_S can be directly obtained from the model. However in most practical PHiL applications the impedance Z_{HuT} of the HuT is not known exactly and is time dependent as well. In this case it can be calculated based on Ohm's law, with a measurement of voltage and current and the $cos(\varphi)$. In case of active and nonlinear load, however, this is far more complicated. Impedance estimation techniques have to be applied, which are described in [5,10].

Due to its simplicity, the PHiL coupling is implemented as voltage type ITM according to Figure 3. The circuit from Figure 7 can be considered as a voltage divider, which is generally known to be stable. However, the interfacing between RTS and HuT provides a time delay and non-ideal behavior which can result in instabilities [11].

3.2. Analytic Stability Analysis

In this section stability of a PHiL simulation will be investigated analytically at the example of voltage type ITM. Therefore the transfer function of a PHiL circuit is analyzed with NSC. A brief introduction to NSC is provided in [6,38].

The voltage type ITM PHiL circuit from Figure 7 can be represented as a block diagram which is shown in Figure 8.

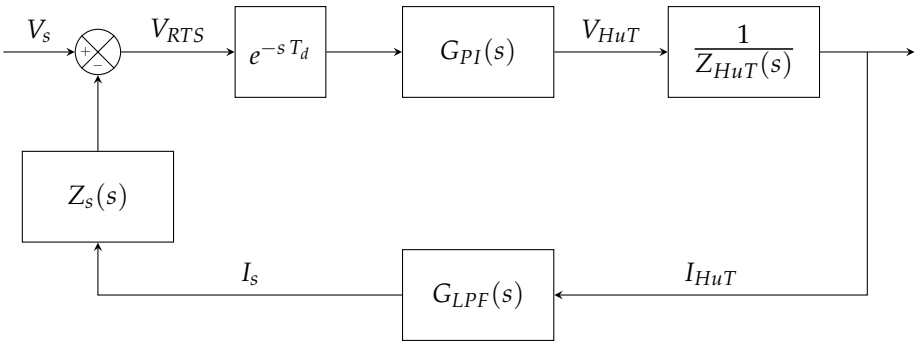

Figure 8. Block diagram of a voltage type ITM PHiL.

The block diagram is implemented in the s-plane. The equivalent grid voltage V_S can be considered as the input of the control loop. All time delays (simulation, communication, amplifier, measurement, etc.) are summed up to a single loop delay time constant T_d. The transfer function $G_{PI}(s)$ of the PI connects to the voltage V_{HuT} at the HuT. An optional low-pass filter $G_{LPF}(s)$ for FSF (see Section 3.2.4) is present in the current feedback path. The OLTF of the PHiL circuit is derived as the product of all blocks within the loop:

$$G_{OLTF}(s) = G_{PI}(s) \cdot G_{LPF}(s) \cdot \frac{Z_S(s)}{Z_{HuT}(s)} e^{-sT_d} \tag{1}$$

In [10] the representation of time delays in PHiL simulation as a polynomial transfer function for treating as an linear time-invariant system is given special focus. However, within the content of this work the exponential representation e^{-sT_d} is sufficient due to the direct applicability in MATLAB™. In the following, stability of the PHiL circuit is analyzed on the basis of the transfer function $G_{OLTF}(s)$.

3.2.1. Resistive Impedance

The circuit in Figure 7 is assumed to be pure resistive with Z_S and Z_{HuT} having only a real component. For simplicity the influence of the amplifier $G_{PI}(s)$ is neglected in this section and FSF is not applied. The simplified OLTF can be rewritten as:

$$G_{OLTF}(s) = \frac{R_S}{R_{HuT}} e^{-sT_d} \tag{2}$$

The resistance R_S and R_{HuT} are assumed to be frequency independent. Figure 9 depicts a locus plot with the quotient of the resistance R_S over R_{HuT} as an additional dimension. With NSC stability margins can be analyzed. In simplified terms, NSC considers a system to be unstable if the Nyquist curve encloses the critical point $(-1, \mathrm{j}\,0)$ in the locus plot of the OLTF [6,7]. The Nyquist curve of the OLTF in Equation (2) describes a circle with radius $\frac{R_S}{R_{HuT}}$ around the origin. Figure 9 therefore forms a funnel-shaped surface. $(-1, \mathrm{j}\,0)$ is marked over the whole range of the impedance ratio as a red line within the figure. Thus, instability is indicated when the critical line intersects the surface. This is the case at a ratio of $\frac{R_S}{R_{HuT}} \geq 1$ (above the blue plane).

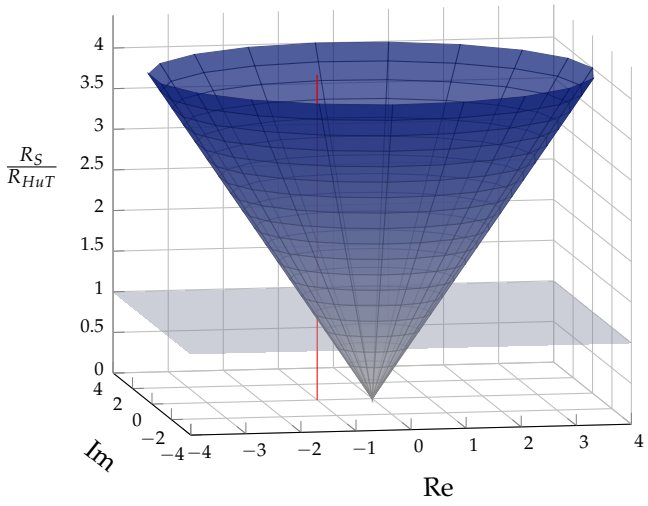

Figure 9. Nyquist curve for resistive impedance PHiL in dependence of the quotient of resistance R_S over R_{HuT}.

The loop delay e^{-sT_d} is frequency dependent, but does not affect the magnitude of the signal. The Nyquist curve in Figure 9 forms a circle around the origin. Thus, a change in phase does not affect the radius of the cycle and therefore has no influence on stability [6]. Figure 10 shows that the radius is not changing, but the number of encirclements until a finite circular frequency.

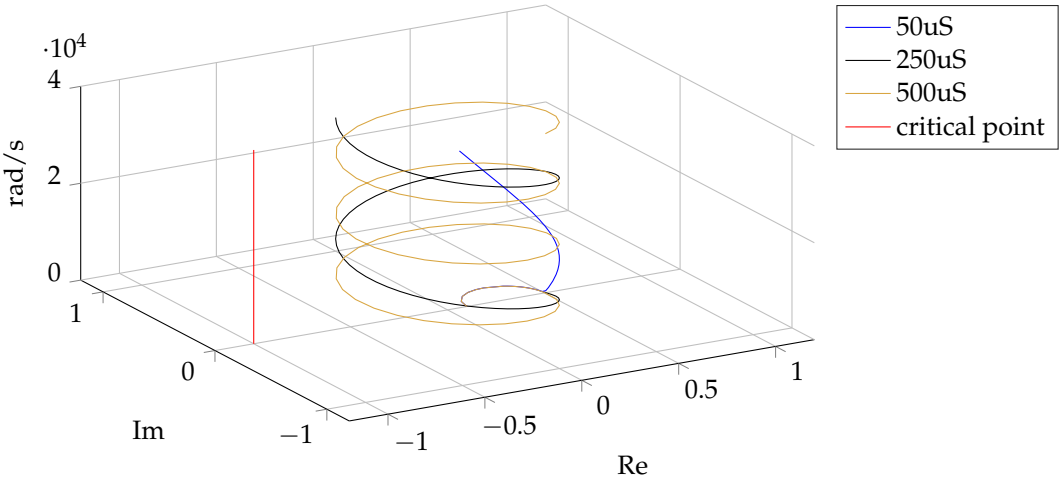

Figure 10. Locus plot with the angular frequency as an additional dimension.

3.2.2. Complex Impedance

The assumption of purely resistive impedances is a very special case. Therefore, in the following, a PHiL simulation with complex impedances Z_S and Z_{HuT} is analyzed.
The OLTF can be expressed as:

$$G_{OLTF}(s) = \frac{R_S + sL_S}{R_{HuT} + sL_{HuT}} e^{-sT_d} \tag{3}$$

Both resistances R_S and R_{HuT} and inductances L_S and L_{HuT} are assumed to be frequency independent.

In the frequency domain the OLTF can be rewritten as:

$$G_{OLTF}(j\omega) = \frac{R_S + (j\omega)L_S}{R_{HuT} + (j\omega)L_{HuT}} e^{-(j\omega)T_d} \tag{4}$$

With frequencies approaching close to zero ($\omega \to 0$), we obtain the previous example with resistive behavior, were the Nyquist curve describes a circle. The center of this circle is zero with a radius of $\frac{R_S}{R_{HuT}}$. Thus, the Nyquist curve starts at the positive real axis at the position $(\frac{R_S}{R_{HuT}}, \mathrm{j}\,0)$.

If frequency, however, points towards infinity ($\omega \to \infty$), the fractional term $\frac{R_S+(j\omega)L_S}{R_{HuT}+(j\omega)L_{HuT}}$ approaches $\frac{L_S}{L_{HuT}}$ whereas the expression $e^{-(j\omega)T_d}$ forms an infinite rotation in mathematically positive direction. Therefore, the locus plot at $\omega \to \infty$ approaches a circle with radius $\frac{L_S}{L_{HuT}}$.

Consequently, both, the ratio of $\frac{R_S}{R_{HuT}}$ and $\frac{L_S}{L_{HuT}}$ have an influence on PHiL stability [6]. In dependence of the ratio of the impedances, three cases are distinguished in the following.

Case A: $R_S \leq R_{HuT}$ and $L_S \leq L_{HuT}$

As explained before the Nyquist curve starts in the point $(\frac{R_S}{R_{HuT}}, j\,0)$ and ends on a circle with radius $\frac{L_S}{L_{HuT}}$. If both the starting and ending points of the locus curve are within the unit circle than the critical point at $(-1, j\,0)$ is never enclosed [6]. According to the NSC this guarantees stability of the PHiL simulation and this is the case, if both, the ratio of $\frac{R_S}{R_{HuT}} \leq 1$ and $\frac{L_S}{L_{HuT}} \leq 1$.

Case B: $R_S \leq R_{HuT}$ or $R_S > R_{HuT}$ and $L_S > L_{HuT}$

In case of $R_S \leq R_{HuT}$ the Nyquist curve starts within the unit circle, respectively if $R_S > R_{HuT}$ the curve starts outside of the unit circle. Due to the ratio of $\frac{L_S}{L_{HuT}} > 1$ the locus curve reaches a circle that encloses the critical point at $(-1, j\,0)$ which makes *Case B* always unstable whenever $L_S > L_{HuT}$. In this case HIA (see Section 2.6.5) could be very efficient.

Case C: $R_S > R_{HuT}$ and $L_S \leq L_{HuT}$

The locus curve starts outside the unit circle in this case, due to $\frac{R_S}{R_{HuT}} > 1$, however, at high angular frequencies $\omega \to \infty$ it approaches a circle with radius $\frac{L_S}{L_{HuT}} \leq 1$ which is inside the unit circle. Whether the critical point at $(-1, j\,0)$ is enclosed by the Nyquist curve (which would make the PHiL simulation unstable), depends on the position of the first root in the left half plane, that is, were the curve intersects the negative real axis the first time [6]. If the first intersection point occurs within the unit circle, i.e., to the right of the critical point, all further intersection points are also within the unit circle. The critical point $(-1, j\,0)$ is therefore never enclosed which results in a stable system. However, if the first intersection appears outside the unit circle, the PHiL is unstable. In [6] a formula is given to examine stability for *Case C* in dependence of the values of R_S, R_{HuT}, L_S and L_{HuT}.

3.2.3. Influence of Time Delay

According to the previous sections, the time delay has no influence on stability within PHiL simulations regarding *Case A* and as long as the impedances are purely resistive. Even at a loop delay which equals a phase shift of 180° in the fundamental frequency a stable PHiL simulation can be achieved [39].

However, regarding *Case C* in Section 3.2.2 time delay can be decisive whether the critical point $(-1, j\,0)$ is enclosed by the Nyquist curve or not.

Apart from stability, time delay has an influence on PHiL simulation accuracy. In voltage type ITM the current in the RTS is determined by the loop-back signal from the measurement of the HuT current. A time delay in the PHiL loop therefore manifests itself as a phase shift between voltage and current in the RTS, which affects the power factor. The loop delay therefore reduces accuracy, since the phase shift results in a reactive power within the RTS which is not present in the HuT [4]. The power factor deviation through loop delay in dependence on system frequency f_s, loop delay T_d and the real active and apparent power flow, that is simulated by the PHiL, can be calculated according to the following equation:

$$cos\varphi_{RTS} = cos(2\pi T_d f_s) \tag{5}$$

In [4], the influence of variable time delays is investigated. Due to the interaction of multiple discrete time systems, a time delay of variable duration can occur, if the discrete systems are not synchronized. This results in an oscillation or noise in the loop-back signal [4].

Noise can be reduced by a low-pass filter (LPF), which commonly has a positive influence on PHiL stability [3].

3.2.4. Stability Improvement with Feedback Signal Filtering

A limitation of the bandwidth of the PHiL loop reduces the accuracy but can have a stabilizing effect on the simulation [3]. A LPF can be implemented in software or in hardware. A software implementation in the feedback loop (see G_{LPF} in Figure 7) makes it a flexible stability improvement with simple implementation without a need for additional hardware [3,23]. The transfer function, a first-order LPF in the s-plane, can be expressed as follows:

$$G_{LPF}(s) = \frac{1}{(1 + \frac{s}{2\pi f_g})} \tag{6}$$

With complex frequency s and the cut-off frequency f_g.

Due to the damping of the amplitude of a signal at frequencies larger than f_g the locus plot will approach the origin $(0, 0)$ at $\omega \to \infty$. Furthermore the phase is increased by the filter. Thus, with decreasing cut-off frequency f_g the radius of the Nyquist curve decreases faster, which stabilizes the system.

Figure 11 displays a locus plot of a voltage-type ITM with an impedance ratio of $R_S > R_{HuT}$ and $L_S > L_{HuT}$, which is unstable according to Section 3.2.2. The diagram is extended by an additional dimension for angular frequency to visualize the effect of band limitation with different cut-off frequencies f_g. From the graph it can be obtained that with $f_g < 1\,\text{kHz}$ a stable PHiL can be achieved.

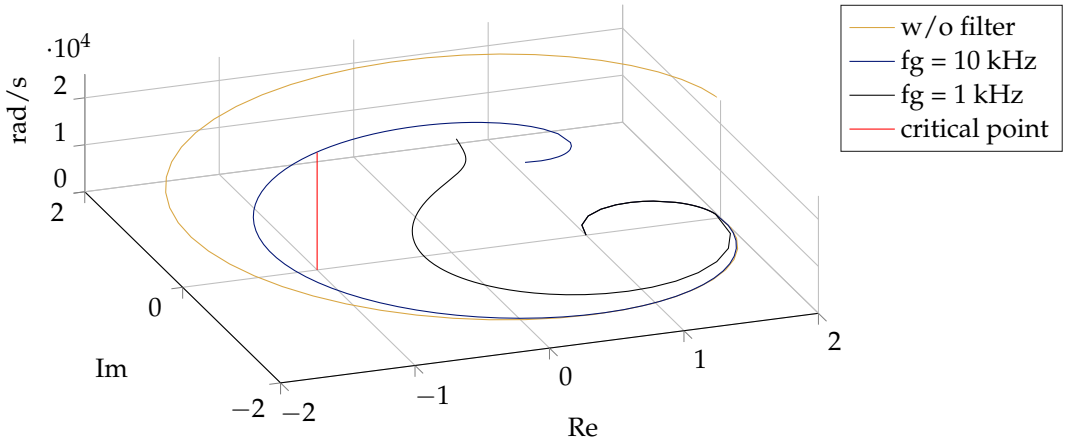

Figure 11. Locus plot of FSF-ITM with different cut-off frequencies with the angular frequency as an additional dimension.

Thus, a LPF can guarantee a stable PHiL simulation even if the impedance ratio would indicate instability, however, at the expense of simulation fidelity and accuracy [14,18]. The design of the current feedback filter should therefore always be a compromise.

3.2.5. Influence of the Power Amplifier

In the previous sections of this paper the influence of the power amplifier was considered as a single time delay. This is very common in literature [12,14]. However, as [11] shows, this simplification results in deviations in comparison to real PHiL simulations. In an ideal case the inverter would be invisible to the HuT. In practice, however, the amplifier output filter as well as the control loop must be included into stability considerations.

In [4,32] a switching inverter is represented as a second order LPF with a time delay. In the same way as FSF, the interfacing amplifier results in band limiting behavior, which leads to an improvement in PHiL stability but also to a deterioration in accuracy.

The current sensors typically have considerably higher bandwidth than the amplifier output filter and control loops and therefore can be neglected [32]. Linear amplifiers, in contrast, provide significantly faster dynamics because converter control and output filters are nearly dispensable. Therefore the transfer function is reduced to a time delay.

In accordance to 3.2.1 and 3.2.2 the total loop delay T_d does not influence stability of PHiL with ITM without band limitation.

However, as soon as low-pass filters are applied a reduction of time delay leads to an increase in phase of the locus plot. Thus, the curve terminates in the origin faster as Figure 12 displays.

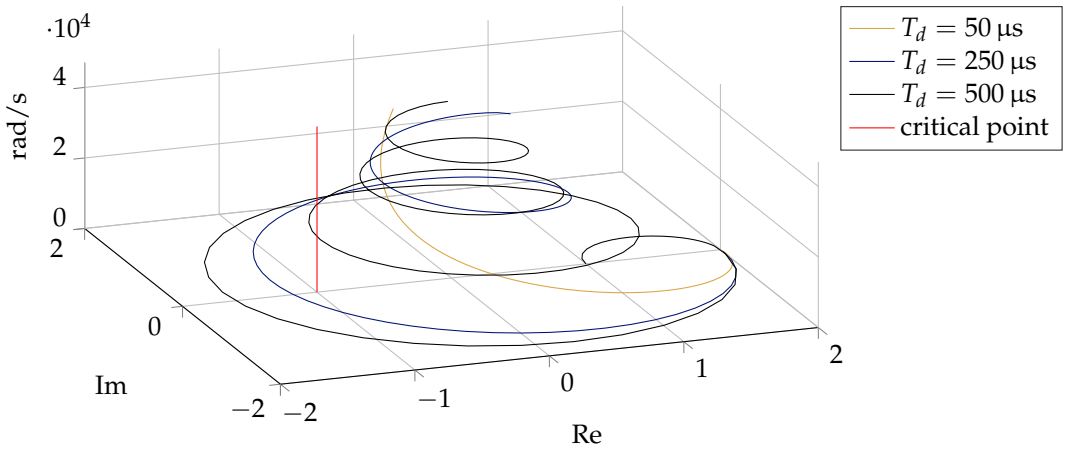

Figure 12. Locus plot of ITM PHiL in dependence of the loop time delay with the angular frequency as an additional dimension.

In Figure 13 the Nyquist curve in the right plot shows identical stability margin of an ITM PHiL simulation with FSF. However, the blue line integrated FSF with a first-order LPF with a cut-off frequency of $f_g = 10\,\text{kHz}$ whereas the orange curve is plotted with a cut-off frequency of $f_g = 2.12\,\text{kHz}$. The difference is due to the simulation step size, which leads to a total loop delay of $T_s = 125\,\mu s$ in the case of the blue line, respectively $T_s = 590\,\mu s$ in case of the orange curve.

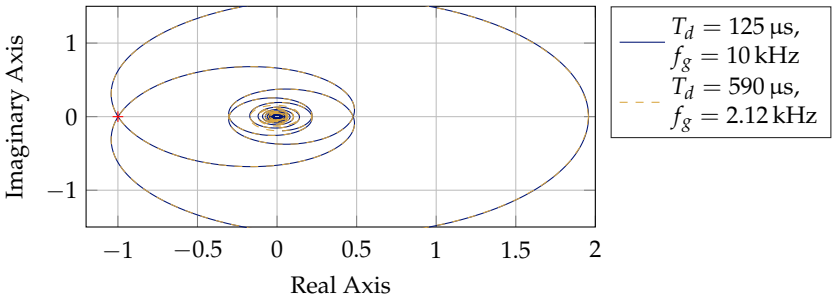

Figure 13. Locus plot of voltage type ITM PHiL with different loop time delays and low pass cut of frequencies.

Consequently a reduction in the loop time delay T_d, through a decrease in simulation sample time or faster power amplifier dynamics, will lead to stability at higher filter cut-off frequencies which in turn improves modeling accuracy.

4. Simulative and Experimental Stability Validation

In this section the findings of the theoretical stability analysis are applied to a PHiL model, which is fully implemented in an offline *emt*-simulation in MATLAB Simulink™, to

verify the theoretical analysis of PHiL stability from the previous section. Following the simulative verification, an experimental validation is done through real PHiL simulations in the *Microgrid, Energy Storage and Power Hardware-in-the-Loop Laboratory* in Section 4.2.

4.1. PHiL Circuit Offline Model

The PHiL circuit depicted in Figure 7 with voltage-type ITM is implemented as an *emt*-model in MATLAB Simulink™ in the discrete z-plane. The implementation of the model is shown in Figure 14.

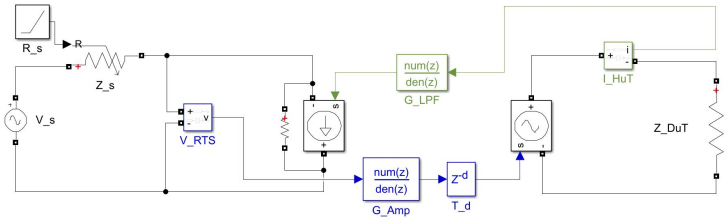

Figure 14. MATLAB Simulink™ model for validation of the stability analysis.

The constant AC-voltage-source V_S with voltage $V_S = 230\,\mathrm{V}$ ($f_S = 50\,\mathrm{Hz}$) supplies the circuit at variable resistor R_S, which can be adjusted during simulation, to examine the stability limit. The impedance Z_{HuT} represents the HuT. According to the voltage type ITM a voltage source at the HuT-side represents an ideal power interface and the feedback current controls a current source with high-resistance bypass branch. The additional impedance in parallel is necessary for solving the equations, however, it can be set to the range of $M\Omega$ which therefore has no influence for the purpose of this study [10]. A transfer function G_{amp} represents the characteristics of the PI and the z^{-d} is the total loop delay. A low-pass filter G_{LPF} for FSF can be integrated into the PHiL circuit. The MATLAB Simulink™ model is discretized and simulated at a time step of $T_a = 62.5\,\mu\mathrm{s}$ in accordance to the PHiL experiment in the following section. Simulation time step size of 50 µs is most common in the field of real time grid simulation [22,27,28]. However, the switching amplifier is operated at 16 kHz, which results in a control time step of 62.5 µs in this case.

4.2. Experimental PHiL Stability Analysis

The analytic and simulative stability analysis from Section 3 is validated in the *Microgrid, Energy Storage and Power Hardware-in-the-Loop Laboratory* in collaboration with the *Real-Time Laboratory* of the LEES. An experimental setup, according to Figure 7, will be analyzed in this section with different PIs: a switching inverter and a linear inverter. The limits of stable operation are measured and will be compared against the simulative and the theoretical approach.

The virtual part of the PHiL circuit is implemented in RSCAD (RSCAD Software Version 5.014.1, RTDS Technologies Inc., Winnipeg, Canada) (see Figure 15) for RTS on a RTDS NovaCor™ real time simulator.

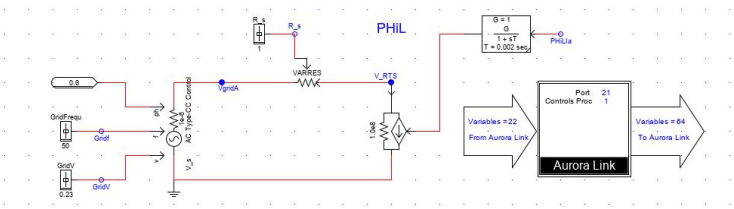

Figure 15. Virtual part of the PHiL simulation modeled in RSCAD.

Both the switching and the linear amplifier are interfaced with the RTS with optical fiber AURORA communication. The HuT is a single phase resistive load with 1.85 kW active power at $cos\varphi = 1$. The resistance is therefore $R_{HuT} = 28.6\,\Omega$.

4.2.1. Experimental Setup with Switching Amplifier

The switching PI is a 4QA from the manufacturer *Triphase NV, Holsbeek, Belgium* with configuration: *PM90I30PM12F120* with a rated power of 45 kVA at the HuT-side and active grid feedback capability (see Figure 16a). The loop delay, that consists of RTS, communication and the delays within the 4QA was measured to an average of 590 µs.

4.2.2. Experimental Setup with Linear Amplifier

For comparison, the setup with the linear inverter is identical, regarding the HuT and RTS model. The linear amplifier is a 4QA of the manufacturer *Spitzenberger & Spies, Viechtach, Germany* of type *DM 15000/APS/PHIL* (see Figure 16b). The three-phase system consists of three synchronized single-phase *APS 5000* amplifier modules as well as a resistor load bank as power sink. The loop time delay of the linear amplifier has been measured to approximately 125 µs, which includes communication and RTS. The same resistive load with $R_{HuT} = 28.6\,\Omega$ is connected as HuT.

(**a**) (**b**)

Figure 16. Four quadrant amplifiers applied in the experimental PHiL setup. (**a**) Switching amplifier; (**b**) Linear amplifier.

4.3. Comparison

The findings of the theoretical stability analysis of Section 3 are applied to the PHiL offline simulations and compared with the results of the practical validation in the following.

4.3.1. Ideal Power Interface

As a first approach, the influence of the power interface (PI) is neglected. An ideal PI with a unity gain of one is assumed. In addition, no FSF is applied. Thus, direct coupling of the RTS and the HuT side with time delay T_d is achieved.

All experiments—simulative and real—in this section will be carried out with a resistive load $R_{HuT} = 28.6\,\Omega$. During simulation in MATLAB Simulink™ the variable resistance R_S is increased until instability of the PHiL simulation occurs. As indicated in [6,18] instability in PHiL simulations appears as distortion and oscillation in the voltage and current waveform. To determine the critical impedance ratio the resistance $R_{S,lim}$ is determined when the PHiL simulation becomes unstable.

According to the NSC instability occurs when the impedance ratio exceeds one: $\frac{R_S}{R_{HuT}} > 1$.

Thus, the system gets unstable if the resistance within the virtual part exceeds $R_{S,lim} = 28.6\,\Omega$. However, within the offline *emt*-simulation in MATLAB Simulink™, as it can be obtained from Figure 17, only at $31.7\,\Omega$ the sine waves signals of voltage and currents are starting to get distorted which indicates instability.

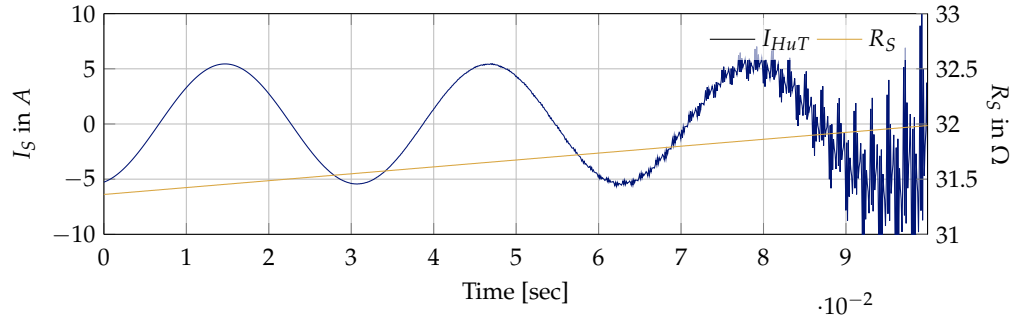

Figure 17. Feedback current with rising R_S until stability limit is reached.

4.3.2. Influence of Amplifier Characteristics

As depicted in Section 3.2.5, the switching amplifier can be represented by a second-order transfer function and a time delay [32]. To characterize the switching amplifier, the step response has been measured, which is shown in Figure 18. A step function V_{RTS} (0–230 V) has been applied within the RTS and is provided at the HuT by the 4QA. The measured voltage at the amplifier terminals V_{HuT} is fed back to the RTS. Both signals (the step function and the measured voltage) have been recorded within the RTS with a sample rate of 62.5 µs.

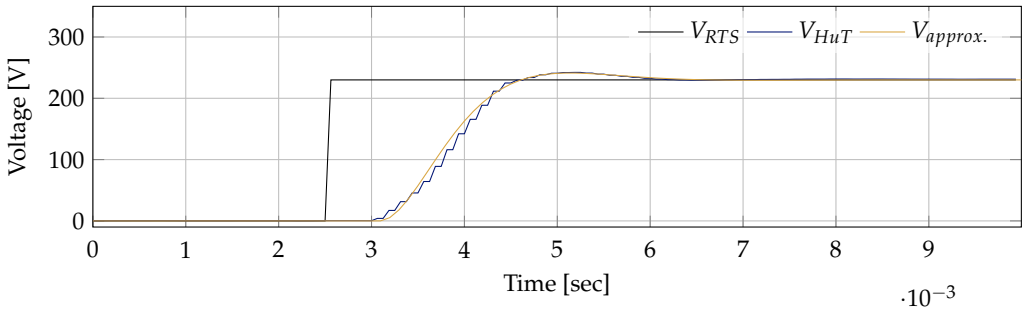

Figure 18. Step response of the switching inverter in comparison to the approximation.

To estimate the characteristics of the amplifier, the step response was approximated with the transfer function of a second order low-pass including a time delay:

$$G_{approx.}(s) = G_{amp}(s) + G_{T_d}(s) = \frac{1}{2.2 \cdot 10^{-7}\, s^2 + 6.5 \cdot 10^{-4}\, s + 1}\, e^{-s \cdot 590\,\mu s} \tag{7}$$

The time delay of 590 µs equals the total round trip delay T_d of the PHiL simulation. The value has been confirmed by further measurements.

One part of the time delay is caused by the control of the converter and measurement delays, whereas another part by the communication and the discrete nature of the RTS. However, since the individual time delays cannot be measured exactly, in this case, the amplifier transfer function $G_{amp}(s)$ and the total time delay $G_{T_d}(s)$ are considered separately in the following.

By application of the amplifier transfer function $G_{amp}(s)$ the band limiting effect of the low-pass characteristics leads to an improvement in PHiL stability. According to NSC, the PHiL circuit can be determined unstable at a resistance ratio of $\frac{R_{RTS}}{R_{HuT}} > 1.57$ ($R_{S,lim} = 44.97\,\Omega$), which is significantly higher than without consideration of $G_{amp}(s)$.

The offline *emt*-simulation in MATLAB Simulink™ indicated instability as $\frac{R_{RTS}}{R_{HuT}} > 1.72$. The experimental PHiL simulation provides a smooth transition between

stable and critically stable operation. Therefore $R_{S,lim}$, is rather a region than a discrete value. With the switching amplifier this is the case at around 47–50 Ω which results in an impedance ration of ≈ 1.7. Only at $R_S > 80\,\Omega$ the PHiL simulation is oscillating as strong as that the PI turns in error mode due to overcurrent limitation.

For comparison the step response of the linear amplifier is shown in Figure 19. Note the finer time resolution in comparison to Figure 18. According to the figure, the transfer function can be reduced to a time delay of two simulation time steps $2\,T_s$.

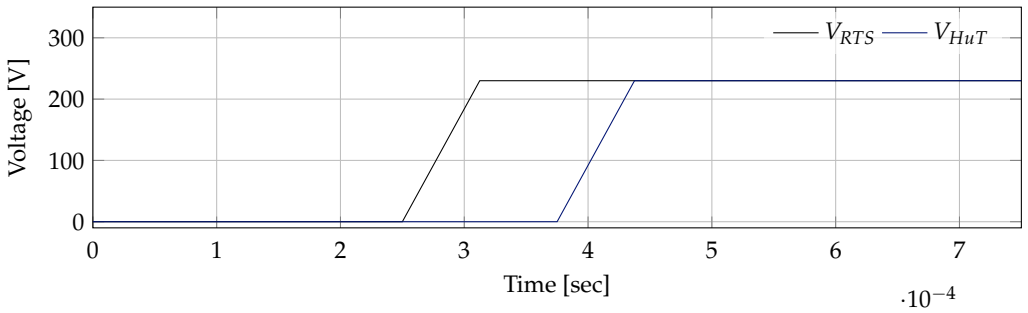

Figure 19. Step response of the linear amplifier.

For noise reduction and anti aliasing the linear amplifier is equipped with a LPF. The filter is a first-order Butterworth low-pass with cut-off frequency $f_g = 1.0\,\text{MHz}$.

Applying Nyquist criterion this would lead to a theoretical ratio of 1.0138. Which is only slightly above ideal interfacing due to the large value of f_g. It should be noted that without additional FSF no stable PHiL simulation could be achieved. A certain noise in the feedback current signal leads to an oscillation during the experiment.

4.3.3. Influence of Feedback Signal Filtering and Time Delay

Further stability improvement can be obtained by the application of a LPF to the current feedback signal, as explained in Section 3.2. With a first-order LPF with $f_g = 1.0\,\text{kHz}$ stability of the circuit with the switching amplifier can be obtained, according to NSC, up to $R_{S,lim} = 61.2\,\Omega$. Whereas, $R_{S,lim} = 94.9\,\Omega$ with filter cut-off frequency $f_g = 0.5\,\text{kHz}$. This is confirmed by the offline *emt*-simulation in MATLAB Simulink™ which indicated instability as $R_{S,lim} > 68.1\,\Omega$ at $f_g = 1.0\,\text{kHz}$ and $R_{S,lim} > 102.8\,\Omega$ at $f_g = 0.5\,\text{kHz}$, resp. A graphical comparison of the results is shown in Figure 20.

Detailed data can be extracted from the Appendix A.

To validate the findings the respective LPF is implemented in the laboratory experiment into the current feedback path within RSCAD.

With filter cut-off frequency $f_g = 1.0\,\text{kHz}$ and $f_g = 0.5\,\text{kHz}$ the current through the HuT gets distorted at an impedance ratio of approximately 2.6 (≈73–77 Ω), and 4.4 (≈122–127 Ω), respectively.

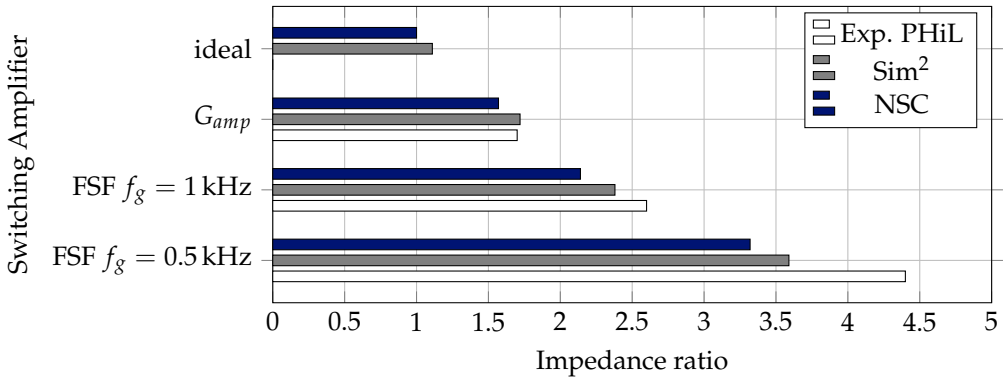

Figure 20. Impedance ratio as stability limit for analysis with a switching inverter.

With the linear inverter substantial extension of stable operation area can be realized by FSF. A LPF with cut off-frequency of $f_g = 1.0\,\text{kHz}$ increases the critical impedance ratio to 13.13 according to NSC. The simulated ratio provides a comparable value of 14.18 whereas the experimental PHiL indicates instability at a ratio greater than 9.08. A graphical comparison of the results with the linear amplifier is shown in Figure 21.

Detailed data can be extracted from the Appendix A.

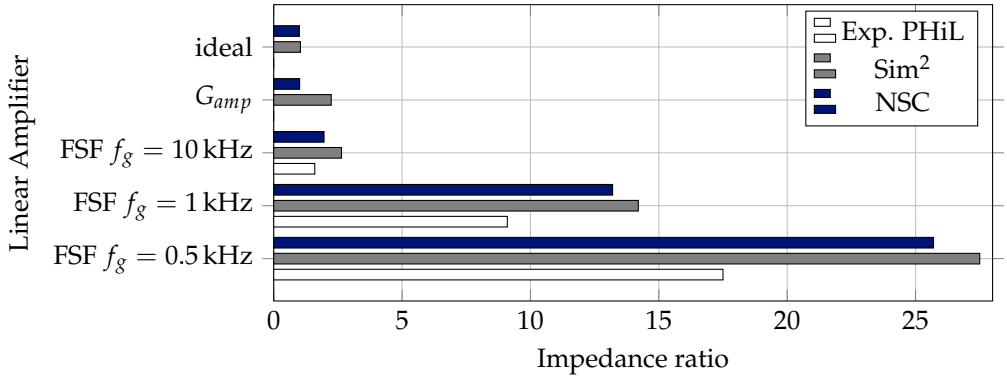

Figure 21. Impedance ratio as stability limit for analysis with a linear inverter.

For investigation of the influence of the loop delay on the power factor, an additional time lag is implemented into the current feedback signal path of the setup with the switchin amplifier. As already explained in Section 3.2.3, a time delay leads to a deviation in the power factor within the RTS.

At minimal loop delay ($T_d = 590\,\mu\text{s}$), a power factor of $cos\varphi = 0.986$ occurs within the RTS in spite of purely resistive R_S and R_{HuT}. In comparison, a power factor of $cos\varphi = 0.983$ can be calculated with Equation (5). Figure 22 compares calculated values of cosphi at several loop time delays with the measured values in the experimental PHiL.

During the experiment, it could be demonstrated that even in case of phase shift of 180° stability is maintained whereas the power factor approaches $cos\varphi = -1$.

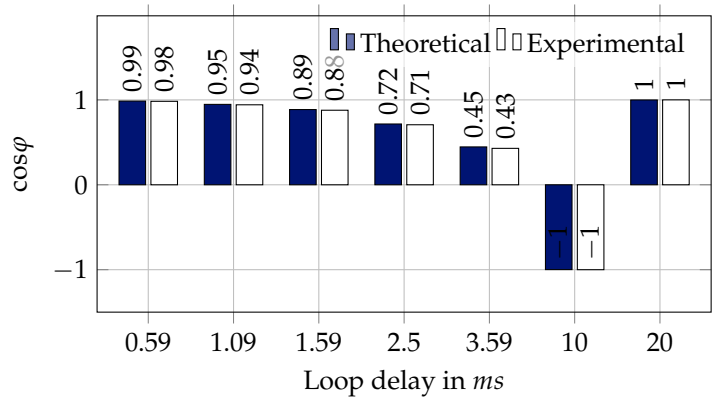

Figure 22. Relation between loop delay and cosphi in comparison between theory and practical PHiL simulation.

5. PHiL for Grid Applications

A PHiL simulation enables the investigation of real physical equipment within simulated electrical power systems as a very flexible and realistic environment.

In the previous sections of this paper, it has been demonstrated, that stability of a PHiL simulation has to be studied carefully based on the ratio of $\frac{Z_S}{Z_{HuT}}$, the loop delay and limitations of bandwidth.

In [10] an impedance analyzer is described for a PV inverter which measures the response of an inverter at a change in grid voltage. In most PHiL simulation applications,

however, the impedance of the HuT is not known exactly and, furthermore, it is changing during the simulation. In addition, the HuT can have nonlinear characteristics, which is the case with power electronic devices.

Thus, in the following, an application of a PHiL simulation will be presented to demonstrate the mitigation of stability issues in practice.

The behavior of a three-phase four-wire low-voltage distribution feeder, similar to the one in Figure 7a, which consist of a residential load and a PV system, shall be investigated. For this reason, the utility grid is replaced by a real-time model for simulation with voltage type ITM PHiL.

All parameters are listed in Table 1. According to the previous sections the impedance ratio of Z_{RTS} to Z_{HuT} is crucial regarding stability. However, Z_{HuT}, which is the total impedance of the PV system in this case, cannot be determined exactly. Furthermore Z_{HuT} is nonlinear and changing during the experiment.

To ensure a stable operation during the whole experiment stability improvements through FSF are implemented.

The household peak load (three-phase) in this example is assumed to be 5.6 kW at $cos\varphi \approx 1$. Thus, the minimal impedance per phase equals $Z_{HuT,min} = 28.6 + \mathrm{j}\,0\,\Omega$. The rooftop PV system consists of a system with a conventional inverter with a rated power of 7 kWp. At the begin of the experiment the PV system is still switched off. Due to the resistive-inductive grid the PHiL simulation would be unstable according to Section 3.2.2 due to $L_{HuT} = 0$ and therefore $L_S > L_{HuT}$. However, with the transfer function of the switching inverter G_{amp} the circuit can be stabilized which can be validated during the experiment.

After the begin of the experiment the PV system is switched on and starts to synchronize with the grid. Although detailed characteristics of the PV inverter are not known, current oscillations can be observed at the moment of synchronization which leads to instability.

To guarantee a stable PHiL simulation, FSF is applied. The application of a first order LPF with cut-off frequency of $f_g = 1$ kHz grantees a stable PHiL simulation. Over the whole operating range of the load and up to 4 kW PV active power (restricted by irradiation during the test) no stability issues were observed.

Although stability is improved through FSF, simulation accuracy diminishes. According to Section 3.2.3 the additional phase shift induced by the LPF influences the power-factor in the RTS. In this exemplary PHiL simulation $T_d = 590\,\mu s$ and the phase shift due to the LPF at the fundamental frequency ($f_s = 50$ Hz) corresponds to 966 µs. Thus, the total shift between voltage in the RTS and the feedback current adds up to 1.56 ms. According to Equation 5 the power factor of the resistive load is reduced to $cos\varphi = 0.88$, which can be confirmed by the experimental PHiL simulation (see Figure 22). A possible mitigation is the introduction of an additional time delay of $T_{comp} = 0.01844\,s$. In Figure 23 the additional time delay T_{comp} is applied at a simulation time of two seconds. Thus, the phase between the simulated voltage V_{RTS} and the feedback current I_S is reduced to zero. Power factor correction through an additional time delay, however, reduces the accuracy of transient events. Therefore [10] presents a filter with a compensator to mitigate phase delay. Another mitigation would be the application of a linear inverter for PI. Due to reduced loop delay with a linear amplifier, stability is guaranteed even if a LPF with higher cut-off frequency is applied, which in turn minimizes power factor deviations.

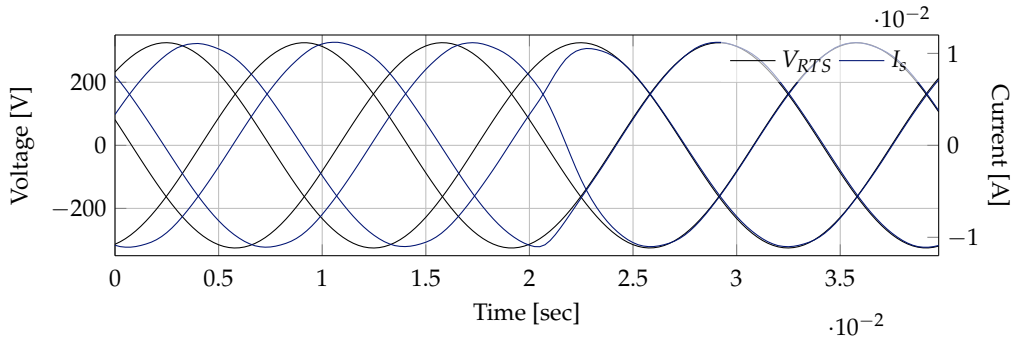

Figure 23. Power factor correction with an additional time delay

Table 1. Parameter of the PHiL application example.

Grid voltage (50 Hz)	V_S	0.4	kV
Grid impedance	Z_{grid}	$100 + \mathrm{j}\,6.3$	$m\Omega$
Load impedance	Z_L	$28.6 + \mathrm{j}\,0$	Ω
LPF cut-off frequency	$f_{g,FSF}$	1.0	kHz
PV system rated power (three phase)	$P_{PV,n}$	7.0	kW

6. Discussion

The comparison of the experimental stability limits match the simulative and theoretical approach. The theoretical limits of $R_{s,lim}$ estimated with NSC are systematically lower than the values from the simulation in MATLAB Simulink™ due to the fact, that NSC analyzes the whole frequency spectrum whereas the *emt*-simulation is restricted to $f_s = 50\,\mathrm{Hz}$. NSC therefore provides a rather pessimistic estimation. Furthermore the values of $R_{s,lim}$ from the laboratory experiment with the switching amplifier exceed the theoretical and simulative results in most cases. This can be explained due to stabilizing features which are included in the inverter control, e.g., harmonics compensation. Accordingly, the resulting impedance ratio with the linear amplifier is lower than anticipated because there is no additional stabilizing control. On the contrary disturbances occur in the laboratory experiment which are not present in simulation.

A comparison of the results with both linear and switching amplifier clearly demonstrates the advantage of reduced time delays and faster simulation time steps.

In the context of this work, estimation of the amplifier transfer function with the step response shows to be sufficient. However, further analysis could be done to improve the knowledge on amplifier characteristics, e.g., frequency behavior and analysis with increased resolution.

The analysis and explanations within this work have been restricted to the voltage type ITM but can easily be extended to current type ITM and other IAs. In [15] both voltage and current type ITM are presented.

Stability improvement with FSF has been demonstrated at the example of a first order low-pass filter as an effective way of improving PHiL stability. However, at the expense of simulation accuracy, as Section 4 could demonstrate, with good accordance between theoretical approach and experimental results. Improved low-pass filter types can reduce the power factor deviation. [10] presents a filter with a compensator to mitigate phase delay.

The experimental verification of the findings from Section 3 has been restricted to a resistive load in Section 4, given the limited frame of this paper, but will be extended to complex impedances in future studies as well as an additional investigation of a nonlinear HuT.

7. Conclusions

In this paper, a general analysis of PHiL stability based on Nyquist stability criterion applied to the transfer function of a simplified circuit has been shown. To the major

influence factors: impedance ratio, time delay, amplifier characteristics and low-pass filtering, special consideration is given. The findings have been applied to an offline model of an exemplary PHiL simulation case, which was implemented in MATLAB Simulink™, to investigate the margin of stable PHiL simulation. The modeling approach was validated with an experimental PHiL setup using a linear and a switching amplifier as power interface in comparison. Apart from a good correlation between theory, simulation and laboratory experiment, the results demonstrate that even inherently unstable PHiL cases can be stabilized with feedback signal filtering method with both, linear and switching inverters. However, due to substantial lower loop delays, linear inverters require less intensive stabilization which has a positive effect on simulation accuracy.

Author Contributions: Conceptualization, S.R.; methodology, S.R.; software, S.R.; validation, S.R.; formal analysis, S.R.; investigation, S.R. (simulation and experimental with switching amplifier) and T.W. (linear amplifier); resources, G.M. (PHiL equipment) and M.L. (Laboratories); data curation, S.R.; writing—original draft preparation, S.R., minor contribution J.F. (Section 2.6); writing—review and editing, S.R., G.M., M.L.; visualization, S.R., minor contribution J.F. (Section 2.6); supervision, S.R.; project administration, S.R., G.M. and M.L.; funding acquisition, M.L. All authors have read and agreed to the published version of the manuscript.

Funding: This work was supported by the Bavarian State Ministry for Education, Culture, Science and Arts (KM) and the DFG.

Institutional Review Board Statement: Not applicable.

Informed Consent Statement: Not applicable.

Data Availability Statement: simon.resch@fau.de.

Conflicts of Interest: The authors declare no conflict of interest.

Abbreviation

The following abbreviations are used in this manuscript:

4QA	Four Quadrant Amplifier
BSS	Battery Storage System
CHiL	Control-Hardware-in-the-Loop
DIM	Damping Impedance Model
DuT	Device unter Test
emt	Electro Magnetic Transient
EUT	Equipment under Test
FAU	Friedrich-Alexander University of Erlangen-Nürnberg
FSF	Feedback Signal Filtering
HIA	Hardware Inductance Addition Method
HiL	Hardware-in-the-Loop
HuT	Hardware under Test
IA	Interfacing Algorithm
ITM	Ideal Transformer Model
LEES	Institute of Electrical Energy Systems
LPF	Low Pass Filter
MRP	Multi-Rate Partitioning Method
NSC	Nyquist Stability Criterion
OLTF	Open Loop Transfer Function
PCC	Point of Common Coupling
PCD	Partial Circuit Duplication
PHiL	Power Hardware-in-the-Loop
PI	Power Interface
PV	Phovoltaic
RTS	Real Time Simulation
TFA	Time-variant First-order Approximation
TLM	Transmission Line Model

Appendix A. Quantitative Data on Stability Limits

Table A1. Comparison of critical impedance ratio with theoretical stability criterion, simulative approach with offline-*emt*-model and practical PHiL simulation with the switching inverter.

Methodology	Plain ITM	G_{amp}, w/o Filter	FSF 1.0 kHz	FSF 0.5 kHz
NSC	1	1.57	2.14	3.32
Simulative approach	1.11	1.72	2.38	3.59
Experimental PHiL	n.a.	1.7	2.6	4.4

Table A2. Comparison of critical impedance ratio with theoretical stability criterion, simulative approach with offline-*emt*-model and practical PHiL simulation with the switching inverter.

Methodology	plain ITM	G_{amp}	FCF 10.0 kHz	FCF 1.0 kHz	FCF 0.5 kHz
NSC	1	1.0138	1.957	13.19	25.73
Sim2	1.044	2.241	2.636	14.18	27.5
Exp. PHiL	n.a.	n.a	1.60	9.08	17.52

References

1. Bruckner, T.; Bashmakov, I.A.; Mulugetta, Y.; Chum, H.; de la Vega Navarro, A.; Edmonds, J.; Faaij, A.; Fungtammasan, B.; Garg, A.; et al. Energy Systems. In *Climate Change 2014: Mitigation of Climate Change. Contribution of Working Group III to the Fifth Assessment Report of the Intergovernmental Panel on Climate Change (IPCC);* Cambridge University Press: Cambridge, UK; New York, NY, USA, 2014.
2. *ISGAN Annex 6 Power T& D Systems—Ancillary Services from Distributed Energy Sources for a Secure and Affordable European system: Main Results from the SmartNet Projects*; 2019. https://www.iea-isgan.org/smartnet (accessed on 20 December 2021).
3. Lauss, G.; Strunz, K. Accurate and Stable Hardware-in-the-Loop (HIL) Real-Time Simulation of Integrated Power Electronics and Power Systems. *IEEE Trans. Power Electron.* **2021**, *9*, 10920–10932.
4. Guillo-Sansano, E.S.; Mazheruddin, H.; Roscoe, A.J.; Burt, G.M.; Coffele, F. Characterization of Time Delay in Power Hardware in the Loop Setups. *IEEE Trans. Ind. Electron.* **2021**, *3* 2703–2713. https://doi.org/10.1109/TIE.2020.2972454.
5. Nzimako, O.; Wierckx, R. *Stability and Accuracy Evaluation of a Power Hardware in the Loop (PHIL) Interface with a Photovoltaic Micro-Inverter*; IECON: Yokohama, Japan, 2015.
6. Wang, S.; Li, B.; Xu, Z.; Zhao, X.; Xu, D. A Precise Stability Criterion for Power Hardware-in-the-Loop Simulation System. In Proceedings of the 10th International Conference on Power Electronics and ECCE Asia, Busan, Korea, 27–30 May 2019.
7. Dolenc, J.; Bozicek, A.; Blazic, B. Stability Analysis of an Ideal-Transformer-Model Interface Algorithm. In Proceedings of the 7th International Youth Conference on Energy, Bled, Slovenia, 3–6 July 2019. https://doi.org/10.1109/IYCE45807.2019.8991575.
8. Riccobono, A.; Helmedag, A.; Berthold, A.; Averous, N. R.; de Doncker, R. W. and Monti, A. Stability and Accuracy Considerations of Power Hardware- in-the-Loop Test Benches for Wind Turbines. *IFAC-PapersOnLine* **2017**, *1*, 10977–10984.
9. Li, F.; Huang, Y.; Wu, F.; Zhang, X.; Zhao, W. Power-Hardware-in-the-Loop Stability Analysis of Inverter. In Proceedings of the 22nd International Conference on Electrical Machines and Systems (ICEMS), Habin, China, 11–14 August 2019. https://doi.org/10.1109/ICEMS.2019.8922536.
10. Pokharel, M.; Ho, C.N.M. Stability Analysis of Power Hardware-in-the-Loop Architecture With Solar Inverter. *IEEE Trans. Ind. Electron.* **2021**, *5* 4309–4319. https://doi.org/10.1109/TIE.2020.2984969.
11. Marks, N. D.; Kong, W. Y. and Birt, D. S.; Stability of a Switched Mode Power Amplifier Interface for Power Hardware-in-the-Loop. *IEEE Trans. Ind. Electron.* **2018**, *11*, 8445–8454.
12. Markou, A.; Kleftakis, V.; Kotsampopoulos, P.; Hatziargyriou, N. *Improving Existing Methods for Stable and More Accurate Power Hardware-in-the-Loop Experiments*; IEEE International Symposium on Industrial Electronics, Institute of Electrical and Electronics Engineers (ISIE): Edinburgh, UK, 2017. https://doi.org/10.1109/ISIE.2017.8001296.
13. Barakos, D.; Kotsampopoulos, P.; Vassilakis, A.; Kleftakis, V. and Hatziargyriou, N. Methods for Stability and Accuracy Evaluation of Power Hardware in the Loop Simulations. In Proceedings of the Mediterranean Conference on Power Generation, Transmission Distribution and Energy Convers(MedPower), Athens, Greece, 2–5 November 2014. https://doi.org/10.1049/cp.2014.1642.
14. Lauss, G.; Lehfuß, F.; Viehweider, A.; Strasser, T. Power Hardware in the Loop Simulation with Feedback Current Filtering for Electric Systems. In Proceedings of the 37th Annual Conference of the IEEE Industrial Electronics Society (IECON 2011), Melbourne, VIC, Australia, 7–10 November 2011. https://doi.org/10.1109/IECON.2011.6119915.
15. Ren, W.; Steurer, M.; Baldwin, T.L. Improve the Stability and the Accuracy of Power Hardware-in-the-Loop Simulation by Selecting Appropriate Interface Algorithms. *IEEE Trans. Ind. Appl.* **2008**, *4*, 1286-–1294.
16. Lamo, P.; de Castro, A.; Sanchez, A.; Ruiz, G.A.; Azcondo, F.J.; Pigazo, A. Hardware-in-the-Loop and Digital Control Techniques Applied to Single-Phase PFC Converters. *Electronics* **2021**, *10*, 1563.

17. Ihrens, J.; Möws, S.; Wilkening, L.; Kern, T.A. and Becker, C. The Impact of Time Delays for Power Hardware-in-the-Loop Investigations. *Energies* **2021**, *14*, 3154, https://doi.org/10.3390/en14113154.
18. Brandl, R. Operational Range of Several Interface Algorithms for Different Power Hardware-in-the-Loop Setups. *Energies* **2017**, *10*, 1946.
19. Kotsampopoulos, P.; Lagos, D.; Hatziargyriou, N.; Faruque, M.O.; Lauss, G.; Nzimako, O.; Forsyth, P.; Steurer, M.; Ponci, F.; Monti, A.; et al. A Benchmark System for Hardware-in-the-Loop Testing of Distributed Energy Resources. *IEEE Power Energy Technol. Syst. J.* **2018**, *3*, 94–103.
20. García-Martínez, E.; Sanz, J.F.; Muñoz-Cruzado, J.; Perié, J.M. A Review of PHIL Testing for Smart Grids—Selection Guide, Classification and Online Database Analysis. *Electronics* **2020**, *3*, 382–405.
21. Edrington, C.S.; Steurer, M.; Langston, J.; El-Mezyani, T.; Schoder, K. Role of Power Hardware in the Loop in Modeling and Simulation for Experimentation in Power and Energy Systems. *Proc. IEEE* **2015**, *12*, 2401–2409.
22. IEEE PES Task Force on Real-Time Simulation of Power and Energy Systems, Real-Time Simulation Technologies for Power Systems Design, Testing, and Analysis. *IEEE Power Energy Technol. Syst. J.* **2015**, *10*, 63–73.
23. Dargahi, M.; Ghosh, A.; Ledwich, G.; Zare, F. Studies in power hardware in the loop (PHIL) simulation using real-time digital simulator (RTDS). In Proceedings of the IEEE International Conference on Power Electronics, Drives and Energy Systems (PEDES), Bengaluru, India, 16–19 December 2012
24. Lehfuss, F.; Lauss, G.; Kotsampopoulos, P.; Hatziargyriou, N.; Crolla, P.; Roscoe, A. Comparison of multiple power amplification types for power Hardware-in-the-Loop applications. In *IEEE Complexity in Engineering (COMPENG)*; IEEE: Piscataway, NJ, USA, 2012; pp. 1–6.
25. Muhammad, M.; Behrends, H.; Geißendörfer, S.; Maydell, K.V.; Agert, C. Power Hardware-in-the-Loop: Response of Power Components in Real-Time Grid Simulation Environment. *Energies* **2021**, *14*, 593.
26. Noureen, S. S.; Shamim, N.; Roy, V. and Bayne, S. B. Real-Time Digital Simulators: A Comprehensive Study on System Overview, Application, and Importance. *Int. J. Res. Eng.* **2017**, 266–277.
27. Kuffel R., Forsyth P. and Peters C., The Role and Importance of Real Time Digital Simulation in the Development and Testing of Power System Control and Protection Equipment. *IFAC-PapersOnLine* **2016**, *27*, 178–182. https://doi.org/10.1016/j.ifacol.2016.10.739.
28. *CIGRE Working Group B4.57, Guide for the Development of Models for HVDC Converters in a HVDC Grid*; 2017. https://e-cigre.org/publication/604 (accessed on 20 December 2021).
29. Nzale, W.; Mahseredjian, J.; Kocar, I.; Fu, X.; Dufour, C. Two Variable Time-Step Algorithms for Simulation of Transients. In Proceedings of the 2019 IEEE Milan PowerTech, Milan, Italy, 23–27 June 2019; pp. 1-6.
30. Resch, S.; Och, S.; Luther, M. In Proceedings of the Conception, Modelling Approach and Practical Implementation of a Hybrid Laboratory-Based Microgrid, NEIS Conference, Hamburg, Germany, 20–21 September 2018.
31. Resch, S.; Luther, M. Reduction of Battery-Aging of a Hybrid Lithium-Ion and Vanadium-Redox-Flow Storage System in a Microgrid Application. In Proceedings of the 2nd IEEE International Conference on Industrial Electronics for Sustainable Energy Systems (IESES), 1–3 September 2020; pp. 80-85.
32. Ren, W. Accuracy Evaluation of Power Hardware-in-the-Loop (PHIL) Simulation. Ph.D. Thesis. Florida State University: Tallahassee, FL, USA, 2007.
33. Haineault, M.; Gregoire, L.A.; Paquin, J.N.; Bélanger, J. *Key Considerations When Selecting Amplifiers for your Power Hardware-in-the-Loop (PHIL) Testbed*; OPAL-RT TECHNOLOGIES Inc.: Montréal, QC, Canada, 2019.
34. García-Martínez, E.; Ballestín, J.; Muñoz-Cruzado, J.; Sanz, J.F. Analysis of a switched and linear power amplifier for Power Hardware-in-the-Loop testing of Smartgrid systems. In Proceedings of the 24th IEEE International Conference on Emerging Technologies and Factory Automation (ETFA), Zaragoza, Spain, 1–10 September 2019.
35. Dmitriev-Zdorov, V. B. Generalized coupling as a way to improve the convergence in relaxation-based solvers. In Proceedings of the EURO-DAC EUROVHDL, Geneva, Switzerland, 16–20 September 1996; pp. 15–20.
36. Hui, S.Y.R.; Fung, K.K.; Christopoulos, C. Decoupled simulation of DC-linked power electronic systems using transmission-line links. *IEEE Trans. Power Electron.* **1994**, *9*, 85–91. https://doi.org/10.1109/63.285497.
37. Dargahi, M.; Ghosh, A.; Ledwich, G. Stability Synthesis of Power Hardware-in-the-Loop (PHIL) Simulation. In Proceedings of the IEEE PES General Meeting, National Harbor, MD, USA, 27–31 July 2014; pp. 1–5. https://doi.org/10.1109/PESGM.2014.6939021.
38. Westphal, L. C. *Handbook of Control Systems Engineering*, 2nd ed.; Springer: Boston, MA, USA, 2018. https://doi.org/10.1007/978-1-4615-1533-3.
39. Tremblay, O.; Fortin–Blanchette, H.; Gagnon, R.; Brissette, Y. Contribution to stability analysis of power hardware–in–the–loop simulators. *IET Gener. Transm. Distrib.* **2017**, *12*, 3073–3079. https://doi.org/10.1049/iet-gtd.2016.1574.